Bipartite networks of oscillators with distributed delays: Synchronization branches and multistability

Nirmal Punetha,[1] Ramakrishna Ramaswamy,[2,3] and Fatihcan M. Atay[4]
[1]*Department of Physics and Astrophysics, University of Delhi, Delhi 110007, India*
[2]*School of Physical Sciences, Jawaharlal Nehru University, New Delhi 110067, India*
[3]*University of Hyderabad, Hyderabad 500 046, India*
[4]*Max Planck Institute for Mathematics in the Sciences, Inselstraße 22, Leipzig 04103, Germany*
(Received 28 December 2014; published 10 April 2015)

We study synchronization in bipartite networks of phase oscillators with general nonlinear coupling and distributed time delays. Phase-locked solutions are shown to arise, where the oscillators in each partition are perfectly synchronized among themselves but can have a phase difference with the other partition, with the phase difference necessarily being either zero or π radians. Analytical conditions for the stability of both types of solutions are obtained and solution branches are explicitly calculated, revealing that the network can have several coexisting stable solutions. With increasing value of the mean delay, the system exhibits hysteresis, phase flips, final state sensitivity, and an extreme form of multistability where the numbers of stable in-phase and antiphase synchronous solutions with distinct frequencies grow without bound. The theory is applied to networks of Landau-Stuart and Rössler oscillators and shown to accurately predict both in-phase and antiphase synchronous behavior in appropriate parameter ranges.

DOI: 10.1103/PhysRevE.91.042906 PACS number(s): 05.45.Ac, 05.45.Pq, 05.45.Xt

I. INTRODUCTION

The bipartite topology describes a connection structure where the nodes of a network can be divided into two groups such that any two nodes that are coupled must belong to different groups. Several of the most commonly studied network topologies, e.g., linear chains, regular grids, rings with an even number of nodes, tree structures, and the star topology, are bipartite [1–7], the simplest instance probably being a pair of nodes connected to each other. Real examples arise in a number of areas of study and Fig. 1(a) shows a schematic depiction of some typical connection topologies. In biology, well-known examples include metabolic networks, the immune system, or gender-related interactions at the species level. In ecology, the food chain and interaction webs can also be bipartite.

The study of network synchronization has found application in many areas of science and technology [8–14] and many of the networks studied in this context frequently fall in the bipartite class. For instance, sequentially coupled lasers (in a chain or on a ring with an even number of elements) [11] or dynamical elements (clocks, cellular populations, lasers, etc.) communicating with each other via a central hub [12] are bipartite networked systems, as is the case of relay-coupled systems, where information is transmitted between two nodes through several intermediate ones [see Fig. 1(b) for a simple case]. In the latter example, each node corresponds to an oscillator and the signal transmission in the system is subject to a time delay τ. The observation that oscillators 1 and 3 can be perfectly phase synchronized while oscillators 1 and 2 and oscillators 2 and 3 are lag synchronized [15] is an example of the interesting spatiotemporal behavior that can arise in relay-coupled bipartite systems. This also underscores the importance of understanding synchronized solutions (both in-phase and antiphase) as a mechanism for bringing about complex temporal correlations in spatially extended systems.

The stability properties of synchronized networks have been considered in earlier work [16–18], which focused upon the completely synchronized in-phase solution. Lag-synchronized states are also important since these correspond to a distinct and useful behavior of the system. In delay-coupled neurons, for example, different synchronized states play an important role in activity patterns, cognition, learning, and pathological conditions [13,14]. With parameter variation, switching has been observed among complete and lag-synchronized states, indicating a transition among different neuronal activities [14]. These findings strengthen the motivation for a detailed exploration of the various synchronized solutions and their stability in bipartite networks.

In this paper our interest is in the nature of synchronization of oscillators on bipartite networks when there is an inherent delay in the coupling. Specifically, we consider a system of N coupled phase oscillators with distributed coupling delays

$$\dot{\theta}_i = \omega + \frac{\varepsilon}{k_i}\sum_{j=1}^{N} a_{ij}\, g\left(\int_0^\infty \theta_j(t-s)f(s)ds - \theta_i(t)\right), \quad i = 1,\ldots,N, \tag{1}$$

where $\theta_i \in S^1$ is the phase of the ith oscillator, ω is the natural frequency of the oscillators, and the coupling function g is a differentiable 2π-periodic function on $\mathbb{R}$. The coupling strength is denoted by ε and details of the connection structure are contained in the numbers $a_{ij} \geqslant 0$, nonzero a_{ij} indicating that there is an input from the jth oscillator to the ith (with a_{ij} not necessarily equal to a_{ji}). The total input received by the ith oscillator is $k_i = \sum_{j=1}^{N} a_{ij}$, which is assumed to be nonzero for all i. The delays in the information transmission between the nodes are represented by the distribution function f, which is assumed to have compact support and satisfy the

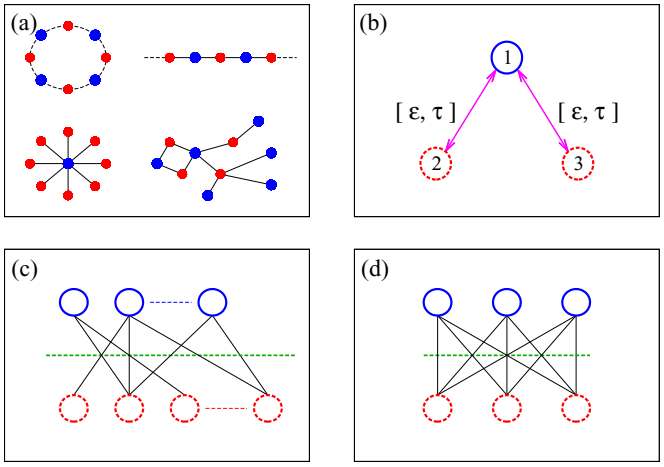

FIG. 1. (Color online) (a) In bipartite networks, the nodes separate into two sets, here marked in red (light gray) and blue (dark gray), such that connections are only between differently colored nodes. (b) Simple example of a bipartite relay network with bidirectional coupling of strength ε and delay τ in the interaction. (c) General coupling scheme in a bipartite topology: In partitions A and B there are N_A and N_B oscillators. The links may be directed. (d) Complete bipartite network with $N_A = N_B = 3$ that has been used in the numerical simulations presented in this paper.

normalization condition

$$\int_0^\infty f(s)ds = 1. \tag{2}$$

Furthermore, the mean delay is defined as

$$\tau = \int_0^\infty s f(s)ds. \tag{3}$$

In the special case when f is given by a Dirac delta function $f(s) = \delta(s - \tau)$, one obtains a discrete delay at the value τ and Eq. (1) becomes

$$\dot{\theta}_i = \omega + \frac{\varepsilon}{k_i}\sum_{j=1}^{N} a_{ij} g(\theta_j(t-\tau) - \theta_i(t)), \quad i = 1, \ldots, N. \tag{4}$$

The undelayed case ($\tau = 0$) with the coupling function $g(x) = \sin x$ has been extensively studied by Kuramoto and coworkers [19] and Crawford [20]. The delayed Kuramoto model was studied by Schuster and Wagner [21], who considered a single pair of oscillators with a discrete delay and numerically investigated their phase-locked solutions. Yeung and Strogatz [17] subsequently studied globally coupled networks in the presence of noise. The effects of delayed feedback on the transition from incoherent to the synchronized state was studied by Goldobin and Pikovsky [22] for an ensemble of globally coupled oscillators. General networks and coupling functions g were investigated by Earl and Strogatz [18], who derived an analytical condition for the stability of the completely synchronized solution under a discrete delay. To restate their result, the synchronized solution $\theta_i(t) = \Omega t\ \forall i$ of Eq. (4), where Ω denotes the common frequency, is locally asymptotically stable if and only if $\varepsilon g'(-\Omega\tau) > 0$.

Despite these fairly extensive studies, the understanding of the dynamics of delay-coupled oscillator networks remains incomplete. For instance, although the criterion of [18] indicates that the synchronized solution of Eq. (4) is unstable when $\varepsilon g'(-\Omega\tau) < 0$, there is no information regarding the actual attractor of the system. Moreover, recent results indicate that there can be a curious spatial organization of coexisting phase-locked and incoherent solutions, namely, the chimera states [23]. These exhibit an even more complex structure when the coupling has time delay [24]. In particular, the neighboring spatial regions of coherence in chimera states have an antiphase relationship with each other, indicating the fundamental importance of in-phase and antiphase synchronization.

Our aim in the present paper is to give a rather complete picture of the synchronized dynamics of Eq. (1) for bipartite networks and thereby extend previous results in several directions. First, we consider phase-locked solutions much like [21] but with a phase difference between partitions (as opposed to between two oscillators) for general coupling functions g and delay distributions f. We show that the only possible values of the phase difference are either zero (corresponding to in-phase, or complete, synchronization) or π radians (corresponding to antiphase synchronization) and derive analytical conditions for the stability of each one. Consequently, we prove that the network switches to an antiphase synchronized state when the synchronization condition given in Refs. [18] is violated: this answers the open question stated above. In this state the oscillators within each partition are completely synchronized with each other, but there is a phase difference of π between the partitions.

Furthermore, by explicitly calculating frequency-delay curves for stable phase-locked solutions, we show that several in-phase and antiphase synchronized states can stably coexist for the same parameter values, each having a different collective frequency. The final behavior of the network is determined only by the initial conditions, i.e., there is multistability. We derive an analytical formula for the number of coexisting stable solutions, which shows that the number of such attractors grows without bound as the mean connection delay increases. Thus, it is possible to essentially *design* a network that has any desired value of the oscillation frequency (within an allowable range that is determined by the coupling strength) by changing the coupling delay; moreover, the partitions can be made to oscillate in-phase or antiphase, as desired. In the final part of this paper we apply the analysis for phase oscillators to coupled limit-cycle and chaotic oscillators, thereby giving a detailed account of synchronization in bipartite networks.

II. SYNCHRONIZATION IN BIPARTITE NETWORKS

When the network underlying Eq. (1) has a bipartite connection structure, the vertex set can be written as the disjoint union of two sets A and B such that $a_{ij} = 0$ whenever i and j both belong to A or both belong to B. We are interested in the synchronized solutions of the network, possibly with a phase difference ϕ between the partitions. Hence, we take

$$\theta_i(t) = \begin{cases} \Omega t & \text{for } i \in A \\ \Omega t - \phi & \text{for } i \in B, \end{cases} \tag{5}$$

where Ω denotes the common synchronous frequency. Substituting into Eq. (1) and using Eqs. (2) and (3), we

obtain

$$\Omega = \omega + \varepsilon g(-\Omega\tau - \phi) = \omega + \varepsilon g(-\Omega\tau + \phi). \quad (6)$$

Thus, a necessary condition for the existence of phase-locked solutions of the form (5) is

$$g(-\Omega\tau - \phi) = g(-\Omega\tau + \phi). \quad (7)$$

Clearly, Eq. (7) always has an in-phase solution $\phi = 0$. We denote the corresponding collective frequency as Ω_0, whose values are given by the solutions of the transcendental equation

$$\Omega_0 = \omega + \varepsilon g(-\Omega_0\tau). \quad (8)$$

In addition, since g is periodic with period 2π, Eq. (7) is also satisfied for $\phi = \pi$. Thus, there can also exist an antiphase solution $\phi = \pi$, with the corresponding frequency Ω_π satisfying

$$\Omega_\pi = \omega + \varepsilon g(-\Omega_\pi\tau - \pi) = \omega + \varepsilon g(-\Omega_\pi\tau + \pi). \quad (9)$$

Moreover, if 2π is the minimum period of g, then $\phi = 0$ and $\phi = \pi$ are the only generic solutions (i.e., solutions that always exist regardless of the value of τ) satisfying Eq. (7). We next show that, for any given values of ω and τ, both Eqs. (8) and (9) have at least one solution for the frequencies Ω and give a condition for the stability of the corresponding synchronous solutions (5).

Theorem 1. Consider Eq. (1) where the delay distribution f has mean value τ and suppose that the network is bipartite and has a spanning tree. Then the following hold.

(a) In-phase solutions. There always exists a solution of the form (5) with $\phi = 0$ and $\Omega = \Omega_0$ given by Eq. (8). Such a solution is locally stable if $\varepsilon g'(-\Omega_0\tau) > 0$ and unstable if $\varepsilon g'(-\Omega_0\tau) < 0$.

(b) Antiphase solutions. There always exists a solution of the form (5) with $\phi = \pi$ and $\Omega = \Omega_\pi$ given by Eq. (9). Such a solution is locally stable if $\varepsilon g'(-\Omega_\pi\tau - \pi) > 0$ and unstable if $\varepsilon g'(-\Omega_\pi\tau - \pi) < 0$.

Furthermore, if g has minimum period 2π, then these are generically the only phase-locked solutions of the form (5).

Proof. We first prove the existence of in-phase and antiphase solutions, that is, solutions to Eqs. (8) and (9), for any given value of intrinsic frequency ω and mean delay τ. Consider the function of Ω_0 defined by the right-hand side of Eq. (8), that is, the mapping $\Omega_0 \mapsto \omega + \varepsilon g(-\Omega_0\tau)$. This function is continuous and bounded on $\mathbb{R}$ (since g is continuous and periodic) and so has a fixed point in $\mathbb{R}$ by intermediate value theorem. Hence, for any given ω and τ, Eq. (8) always has a solution Ω_0. By a similar argument, Eq. (9) always has a solution Ω_π. Now, to determine the stability of solutions of the type (5), consider small perturbations u_i around it, i.e.,

$$\theta_i(t) = \begin{cases} \Omega t + u_i(t), & i \in A, \\ \Omega t - \phi + u_i(t), & i \in B. \end{cases} \quad (10)$$

Substituting into Eq. (1) yields the linear variational equation

$$\dot{u_i}(t) = \begin{cases} g'(-\Omega\tau - \phi)\frac{\varepsilon}{k_i}\sum_{j\in B} a_{ij}\left(\int_0^\infty u_j(t-s)f(s)ds - u_i(t)\right) & \text{for } i \in A \\ g'(-\Omega\tau + \phi)\frac{\varepsilon}{k_i}\sum_{j\in A} a_{ij}\left(\int_0^\infty u_j(t-s)f(s)ds - u_i(t)\right) & \text{for } i \in B, \end{cases} \quad (11)$$

where the prime indicates the derivative. Note that since g is a periodic function of period 2π, so is its derivative g'; thus for ϕ equal to either 0 or π one has $g'(-\Omega\tau - \phi) = g'(-\Omega\tau + \phi)$. Consequently, Eq. (11) can be written as a single expression

$$\dot{u_i}(t) = \beta\frac{1}{k_i}\sum_{j=1}^{N} a_{ij}\left(\int_0^\infty u_j(t-s)f(s)\,ds - u_i(t)\right), \quad i = 1,\ldots,N, \quad (12)$$

where $\beta = \varepsilon g'(-\Omega\tau - \phi) = \varepsilon g'(-\Omega\tau + \phi)$. If $\beta > 0$ and the network has a spanning tree, then Theorem 4.2 of [25] implies that solutions of (12) satisfy $\lim_{t\to\infty} u_i(t) = c$ for some constant c and all i. Therefore, the oscillator phases (10) approach again a solution of the form (5), which proves the stability statement.

It remains to show the instability of (12) when $\beta < 0$. By direct construction it can easily be seen that (12) has a diverging solution. Hence we take

$$u_i(t) = \begin{cases} e^{\lambda t} & \text{for } i \in A \\ -e^{\lambda t} & \text{for } i \in B. \end{cases} \quad (13)$$

Substitution into Eq. (12) gives

$$\lambda = -\beta(1 + F(\lambda)), \quad (14)$$

where $F(\lambda) = \int_0^\infty e^{-\lambda s} f(s)ds$ is the Laplace transform of f. We show that Eq. (14) has a real solution $\lambda > 0$ and thus Eq. (13) is a diverging solution to (12). To this end, consider the right-hand side of Eq. (14) as a real-valued function $H(\lambda) := -\beta(1 + F(\lambda))$ defined on $[0,\infty)$. Since by assumption $\beta < 0$ and by Eq. (2) $|F(\lambda)| \leqslant 1$ for $\lambda \geqslant 0$, we have $0 \leqslant H(\lambda) \leqslant 2|\beta|$ for $\lambda \geqslant 0$. Thus H is a continuous function mapping the interval $[0, 2|\beta|]$ into itself. It follows by Brouwer's fixed-point theorem that H has a fixed point in $[0, 2|\beta|]$, namely, a solution $\lambda \geqslant 0$ to (14). Finally note that $\lambda \neq 0$ since $H(0) = -2\beta \neq 0$ and thus there must be a solution to (12) of the form (13) with some $\lambda > 0$. This completes the proof. ■

Note that the theorem above gives a set of conditions for the stability of both in-phase and antiphase solutions, one or more of which may be simultaneously satisfied. Specifically, in-phase solutions with frequency Ω_0 are stable if

$$\varepsilon g'(-\Omega_0\tau) > 0 \quad (15)$$

and antiphase solutions with frequency Ω_π are stable whenever

$$\varepsilon g'(-\Omega_\pi\tau + \pi) > 0, \quad (16)$$

where Ω_0 and Ω_π are solutions of the transcendental equations (8) and (9), respectively. It is possible that Eqs. (8) and (9) have multiple solutions and both Eqs. (15) and (16) are satisfied for a given set of parameter values, suggesting a rich structure

of coexisting in-phase and antiphase synchronous solutions with different frequencies. In the next section we will present details of this multistable behavior.

III. MULTISTABILITY OF SYNCHRONIZED SOLUTIONS IN KURAMOTO OSCILLATORS

The complex structure of synchronized solutions can be illustrated for the case $g(x) = \sin(x)$, namely, a bipartite network of Kuramoto oscillators [19]

$$\dot{\theta}_i = \omega + \frac{\varepsilon}{k_i} \sum_{j=1}^{N} a_{ij} \sin\left(\int_0^\infty \theta_j(t-s) f(s) ds - \theta_i(t) \right). \tag{17}$$

The condition (6) for the existence of phase-locked solutions takes the form

$$\sin(-\Omega\tau - \phi) = \sin(-\Omega\tau + \phi), \tag{18}$$

which simplifies to

$$\sin(\phi)\cos(\Omega\tau) = 0, \tag{19}$$

and thus in the generic case the only possible phase-locked solutions are in phase or antiphase (namely, $\phi = 0$ or π). By Eqs. (8) and (9), the collective frequencies are given by the roots of the transcendental equations

$$\begin{aligned} \Omega_0 &= \omega - \varepsilon \sin(\Omega_0 \tau) \quad \text{for in-phase solutions,} \\ \Omega_\pi &= \omega + \varepsilon \sin(\Omega_\pi \tau) \quad \text{for antiphase solutions.} \end{aligned} \tag{20}$$

Following Eqs. (15) and (16), the in-phase synchronized solution will be stable when

$$\varepsilon \cos(\Omega_0 \tau) > 0, \tag{21}$$

while the antiphase synchronized solution will be stable when

$$\varepsilon \cos(\Omega_\pi \tau) < 0. \tag{22}$$

For numerical calculations we use a complete bipartite network with $N_A = N_B = 3$ [see Fig. 1(d)], normalize the intrinsic frequency to $\omega = 1$, and start from random initial conditions. Furthermore, it suffices to consider a fixed discrete delay τ, i.e., $f(s) = \delta(s - \tau)$, since the stability condition given in Theorem I depends only on the mean value of the delay.

Figure 2 shows numerical and analytical results [from Eqs. (20)–(22)] for the stable in-phase and antiphase solutions. Note that there are ranges of τ where only a single frequency is stable, as well as ranges of τ where several frequencies correspond to stable motion. The latter multistable regions are indicated by dashed boxes and, as can be seen, the width of these regions of multistability increases with increasing delay τ. For larger coupling, multistability can be observed for even fairly small delays [Fig. 2(c)].

The agreement between numerical simulations and the results of the analysis in Eqs. (20)–(22) is generally excellent. Regions of different dynamical behavior in the ε-τ plane are shown in Fig. 3. Multistability that is seen in this system is an important effect of time delays and becomes even more pronounced at higher values of τ and ε: Figure 4 shows that the number of stable in-phase and antiphase solutions increases as a function of delay and coupling strength. The

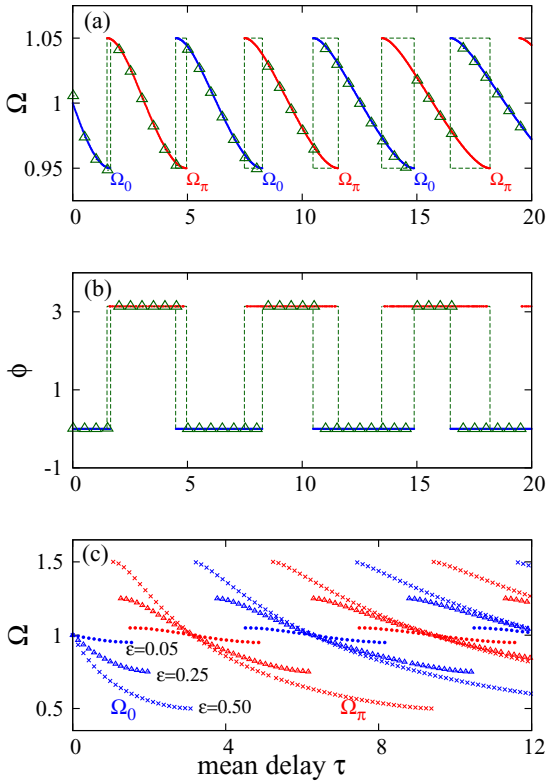

FIG. 2. (Color online) (a) Frequencies of stable phase-locked solutions of coupled Kuramoto oscillators (17), as given by Eq. (20) as a function of the mean delay τ (we set $\varepsilon = 0.05$). (b) Corresponding phase difference between the partitions, which is either zero or π. The blue (dark gray) and red (light gray) curves correspond to in-phase Ω_0 and antiphase Ω_π solutions, respectively. Their overlaps, shown by dashed boxes in (a) and (b), indicate regions of multistability. Simulation results from the system (17), shown by green triangles, for frequencies and phase differences between the two partitions are matched with analytical results in (a) and (b), respectively. (c) Variation of the frequencies with the coupling strength, calculated from Eq. (20), for $\varepsilon = 0.05$ (dots), 0.25 (triangles), and 0.5 (crosses).

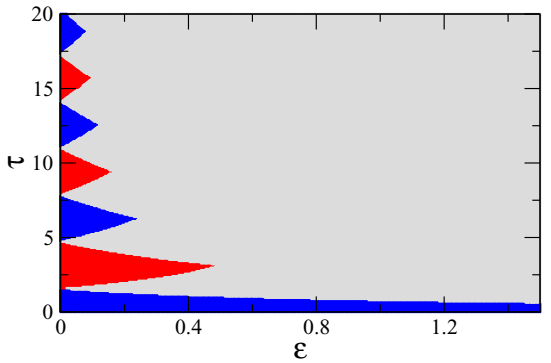

FIG. 3. (Color online) Dynamical phase diagram as a function of the parameters ε and τ. In the blue (dark gray) regions, only in-phase synchronized solutions are stable, whereas in the red (medium gray) regions only antiphase solutions are stable. In the gray (light gray) region there is multistability with several in-phase and antiphase solutions coexisting.

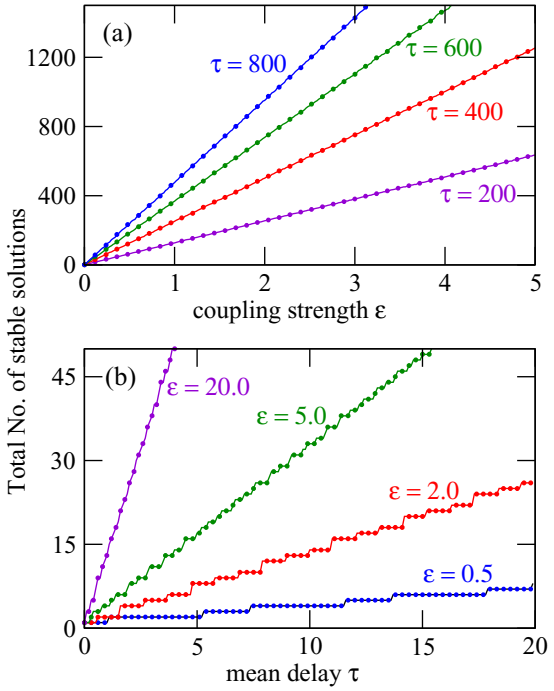

FIG. 4. (Color online) Variation of the number of stable in-phase and antiphase solutions as a function of (a) coupling strength ε and (b) mean delay τ.

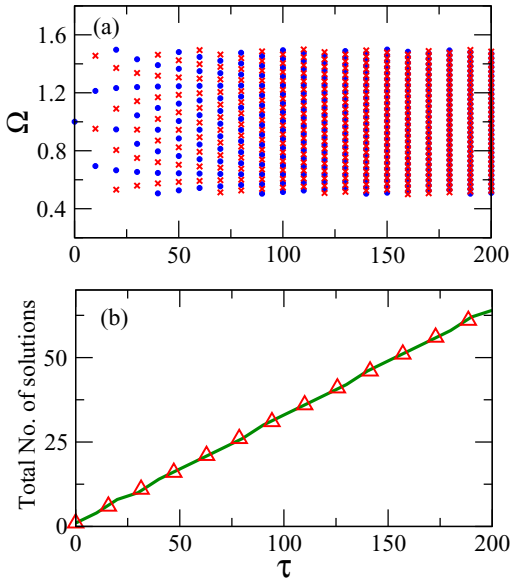

FIG. 5. (Color online) Variation of the number of stable solutions as a function of the time delay, at a fixed coupling strength $\varepsilon = 0.5$. In (a), the blue dots indicate in-phase and the red crosses antiphase solutions. The range of solutions remain bounded in the range from $1-\varepsilon$ to $1+\varepsilon$, while the number of solutions increases with the delay as shown by solid green line in (b). The number of solutions (shown as red triangles) are calculated by counting the intervals satisfying Eqs. (26) and (27) for delay values $\tau = n\pi/\omega$, $n = 1,2,\ldots$ (details in Sec. IV).

increase is essentially linear (modulo the fact that the number of solutions must jump between integer values), so the number of stable solutions can be made *arbitrarily* large, whereas the possible values of the collective frequency Ω are bounded since by Eq. (20),

$$|\Omega - \omega| \leqslant |\varepsilon| \tag{23}$$

for both in-phase and antiphase solutions.

While the coupling strength puts a bound on the deviation of the synchronous frequency Ω from the intrinsic one ω, the time delay only affects the actual value of Ω within the bound. For a fixed coupling strength ε, on the other hand, increasing the delay increases the number of stable solutions within the frequency interval given by Eq. (23), as can be seen in Fig. 5. In this manner, the time delay effectively acts as a frequency selector in a range that is determined by the coupling strength.

However, as the number of stable solutions increases, their domains of attraction become smaller and the actual oscillation frequency of the coupled system becomes more sensitive to external perturbations (see Fig. 6). Under such circumstances, as may be anticipated, the system exhibits hysteresis when system parameters (e.g., the delay) are increased and then decreased back to their original value (see Fig. 7).

IV. ANALYTIC FORMS FOR SOLUTION BRANCHES

In this section we present the analytical basis for the numerical observations of Sec. III. Setting $g(x) = \sin x$, from Eq. (8) we have for in-phase solutions

$$\tau = -\frac{1}{\Omega_0}\arcsin\left(\frac{\Omega_0 - \omega}{\varepsilon}\right) \tag{24}$$

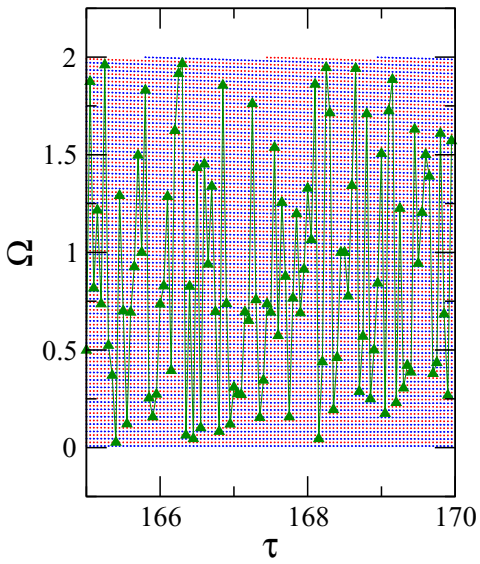

FIG. 6. (Color online) Numerically computed frequencies (green triangles) of the Kuramoto oscillators plotted as a function of delay τ at coupling strength $\varepsilon = 1.0$. We take a complete bipartite network with $N_A = N_B = 3$. The analytically computed frequencies (in-phase and antiphase) are represented by the dots. A large number of stable frequencies have values very close to each other and depending on initial conditions the system settles into one of these in the range $[1-\varepsilon, 1+\varepsilon] = [0,2]$.

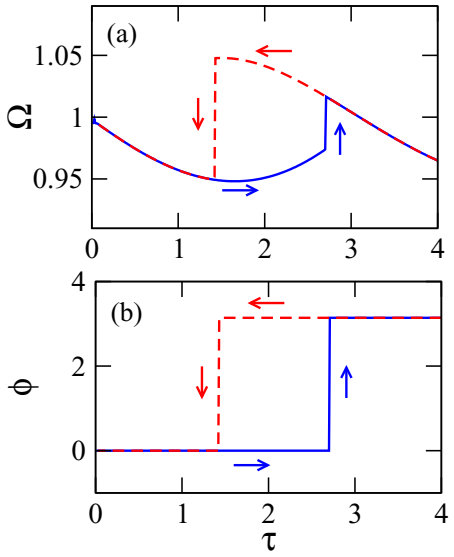

FIG. 7. (Color online) Hysteresis curves in the multistability regime. (a) Collective frequency Ω and (b) phase difference ϕ when τ is varied in steps of $\delta\tau$ from 0 to 4 and in steps of $-\delta\tau$ from 4 to 0 ($\delta\tau = 0.01$, $\varepsilon = 0.05$).

and from Eq. (9) for antiphase solutions

$$\tau = -\frac{1}{\Omega_\pi}\left[\arcsin\left(\frac{\Omega_\pi - \omega}{\varepsilon}\right) + \pi\right]. \tag{25}$$

Since the argument of the arcsin is restricted to the range $[-1,1]$, this gives $(\omega - \varepsilon) < \Omega_{0,\pi} < (\omega + \varepsilon)$. (We assume $\omega > \varepsilon$ for simplicity.) Over this range of Ω, the relation given by Eqs. (24) and (25) can be plotted on the Ω-τ plane, yielding curves similar to those shown in Fig. 8 [cf. Fig. 2(a)]. The figure actually depicts only the stable solutions, which are determined as follows. By Theorem I, the in-phase solution is stable for $\varepsilon\cos(\Omega_0\tau) > 0$, namely, for $-\frac{\pi}{2} + 2k\pi < \Omega_0\tau < \frac{\pi}{2} + 2k\pi$, with $k \in \mathbb{N}$. Using the limits on Ω, this gives the range of τ

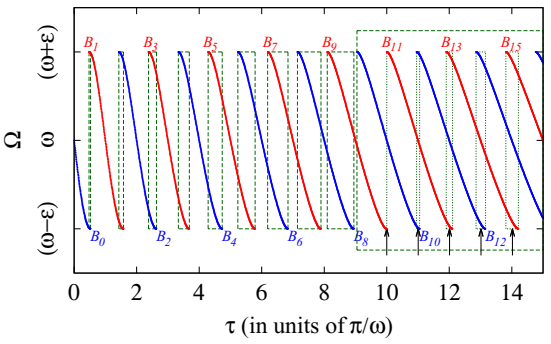

FIG. 8. (Color online) Collective synchronous frequency Ω (vertical axis) from Eqs. (24) and (25) plotted against the mean delay τ (horizontal axis). Stable solution branches are indicated by B_n, where even and odd values of n indicate in-phase and antiphase branches, respectively. The dashed boxes are the region of multistability and the dotted boxes, indicated by the arrows, show the highest number of overlaps, three overlapping branches in this case.

for the stable in-phase solution as

$$\frac{\pi}{\omega+\varepsilon}\left(-\frac{1}{2} + 2k\right) < \tau < \frac{\pi}{\omega-\varepsilon}\left(\frac{1}{2} + 2k\right). \tag{26}$$

For every $k \in \mathbb{N}$ there is a branch of in-phase solutions, shown by the blue curves in Fig. 8. A similar calculation gives the range of τ for stable antiphase solutions as

$$\frac{\pi}{\omega+\varepsilon}\left(-\frac{1}{2} + (2k+1)\right) < \tau < \frac{\pi}{\omega-\varepsilon}\left(\frac{1}{2} + (2k+1)\right), \tag{27}$$

shown by the red curves in Fig. 8. Combining Eqs. (26) and (27), we obtain branches of stable solutions B_n in the Ω-τ plane: On each branch, τ varies over the interval

$$I_n := \left(\frac{\pi(n-1/2)}{\omega+\varepsilon}, \frac{\pi(n+1/2)}{\omega-\varepsilon}\right) \tag{28}$$

and Ω is uniquely defined by the solution of Eqs. (8) and (9). Even and odd values of n correspond to in-phase and antiphase solution branches, respectively.

Note that the length of the interval I_n equals

$$\pi n\left(\frac{2\varepsilon}{\omega^2-\varepsilon^2}\right) + \pi\left(\frac{\omega}{\omega^2-\varepsilon^2}\right). \tag{29}$$

Furthermore, the point $\tau_n := n\pi/\omega$ belongs to I_n for all $n \in \mathbb{N}$ (corresponding to the frequency $\Omega = \omega$). The branches start overlapping with increasing n since the points $\{n\pi/\omega\}_{n\in\mathbb{N}}$ are equally spaced on the real line, but the length of I_n increases linearly with n. We can determine the number of overlaps as follows. Clearly, branch B_n overlaps branch B_{n+m} when the right end point of the former exceeds the left end point of the latter. By Eq. (28), the condition is

$$\frac{n+1/2}{\omega-\varepsilon} \geqslant \frac{n+m-1/2}{\omega+\varepsilon},$$

which, after rearranging, gives

$$m \leqslant \frac{2\varepsilon n + \omega}{\omega^2-\varepsilon^2}.$$

Since m must be an integer, we arrive at the formula for the number of overlaps m:

$$m = \left\lfloor \frac{2\varepsilon n + \omega}{\omega^2-\varepsilon^2} \right\rfloor, \tag{30}$$

where $\lfloor\cdot\rfloor$ denotes the floor function, i.e., the largest integer less than or equal to its argument. Equation (30) shows that the number of overlaps m increases linearly with n. As noted above, we have $\tau_n = n\pi/\omega \in I_n$. Therefore, the number of coexisting stable synchronized solutions increases essentially linearly with increasing mean delay τ and grows unbounded [cf. Fig. 4(b)]. (The number of overlaps of the branches B_n does not always strictly increase with τ, as can be seen from Fig. 8, hence the phrase "essentially linear.") Shown in Fig. 8 are several windows of multistability (the dashed green boxes). With increasing mean delay, the width of these windows increases linearly.

The discussion above applies also for general differentiable coupling functions g and not only for the sine function that we have used for definiteness. Indeed, restricting attention

to domains over which g is strictly increasing or strictly decreasing, one finds intervals on which g can be inverted, thus obtaining solution branches on which

$$\tau = -\frac{1}{\Omega_0} g^{-1}\left(\frac{\Omega_0 - \omega}{\varepsilon}\right)$$

or

$$\tau = -\frac{1}{\Omega_\pi}\left[g^{-1}\left(\frac{\Omega_\pi - \omega}{\varepsilon}\right) + \pi\right],$$

similar to Eqs. (24) and (25). The stability can be checked using Theorem I and the remainder of the analysis proceeds in an analogous manner.

V. APPLICATIONS TO COUPLED LIMIT-CYCLE AND CHAOTIC OSCILLATORS

The analysis carried out in the preceding sections has a wider range of application, beyond coupled phase oscillators. As is well known, it is sometimes possible to define appropriate phase variables for coupled higher-dimensional limit cycle or even chaotic oscillators that, under suitable approximations for the amplitudes, are governed by equations of the form (1). In this section we use these ideas to deduce the behavior of bipartite networks of delay-coupled limit cycle and chaotic oscillators.

A. Landau-Stuart oscillators

The Landau-Stuart system is a simple limit-cycle oscillator that can be viewed as a normal form for the Hopf bifurcation. The equations of motion for such oscillators coupled with time delay are given by

$$\dot{Z}_i = (A + i\omega - |Z_i|^2)Z_i + \frac{\varepsilon}{k_i}\sum_{j=1}^{N} a_{ij}(Z_j(t-\tau) - Z_i), \tag{31}$$

where $Z_k = x_k + iy_k$ is a complex variable, ω is the intrinsic frequency of the oscillators, and ε is the coupling strength. We set the parameter $A = 1$ for numerical calculations. Following the reduction procedure [26] by transforming Eq. (31) into polar coordinates $\theta_i = \arctan(y_i/x_i)$ and $R_i = \sqrt{x_i^2 + y_i^2}$, we obtain the following equations for the amplitudes:

$$\dot{R}_i = R_i\left(1 - \varepsilon - R_i^2\right) + \frac{\varepsilon}{k_i}\sum_{j=1}^{N} a_{ij} R_j(t-\tau)\cos[\theta_j(t-\tau) - \theta_i] \tag{32}$$

and the phases

$$\dot{\theta}_i = \omega + \frac{\varepsilon}{k_i}\sum_{j=1}^{N} a_{ij}\frac{R_j(t-\tau)}{R_i(t)}\sin[\theta_j(t-\tau) - \theta_i]. \tag{33}$$

When the amplitudes are nearly equal, namely, $R_i/R_j \approx 1$, the equations for the evolution of oscillator phases reduce to the standard Kuramoto form and we find the reduced phase equation

$$\dot{\theta}_i = \omega + \frac{\varepsilon}{k_i}\sum_{j=1}^{N} a_{ij}\sin[\theta_j(t-\tau) - \theta_i]. \tag{34}$$

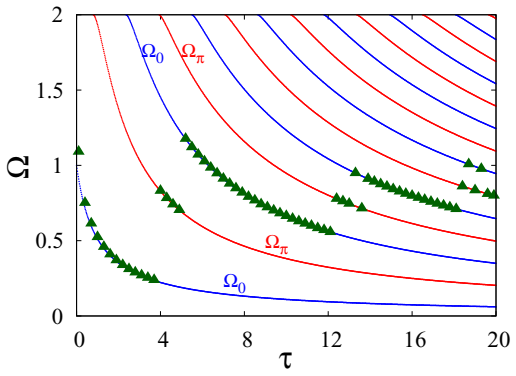

FIG. 9. (Color online) Variation of frequencies with mean delay in coupled Landau-Stuart oscillators on a bipartite network ($N_A = N_B = 3$). Blue and red lines (indicated by Ω_0 and Ω_π) are, respectively, the in-phase and antiphase frequencies calculated from the transcendental equations (20) at $\varepsilon = 1.0$. Green triangles are the numerically calculated frequencies from the system (31).

The phase dynamics of the coupled Landau-Stuart system (31) is therefore identical to that of the Kuramoto system (17) for the same values of ε and τ (see Figs. 9 and 10). The phase-locked solutions can have a phase difference of $\phi = 0$

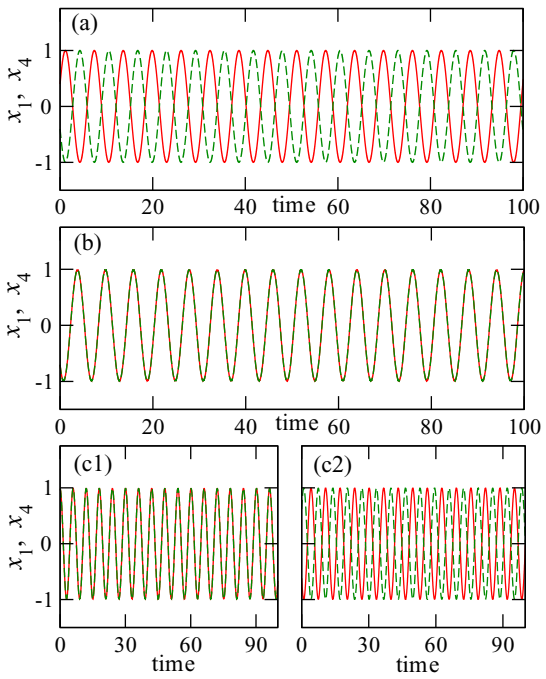

FIG. 10. (Color online) Behavior of coupled Landau-Stuart oscillators on a bipartite network ($N_A = N_B = 3$) for coupling strength $\varepsilon = 0.05$. After removing transients, the variable $x(t)$ for oscillators $i = 1 \in A$ (solid red line) and $i = 4 \in B$ (dashed green line) is plotted as a function of time. The behavior of the system is identical to that of coupled Kuramoto oscillators at the same parameter values. (a) At $\tau = 3.0$, the oscillators from different partitions are antiphase synchronized. (b) At $\tau = 5.0$, the oscillators from different partitions are in-phase synchronized. (c) Oscillators show multistable behavior at $\tau = 17.0$. Here two different initial conditions lead to (c1) in-phase and (c2) antiphase states.

or π and the collective frequencies satisfy Eq. (20) as before. Figure 9 shows that the analytically calculated frequencies from Eq. (20) are in very good agreement with numerical results. Furthermore, it is straightforward to see when the coupled system exhibits in-phase or antiphase synchrony, as shown in Fig. 10.

B. Rössler oscillators

For chaotic Rössler oscillators diffusively coupled (via the variable x) with time delay, the equations of motion are

$$\begin{aligned}\dot{x}_i &= -\omega y_i - z_i + \frac{\varepsilon}{k_i}\sum_{j=1}^{N} a_{ij}(x_j(t-\tau) - x_i(t)),\\ \dot{y}_i &= -\omega x_i + a y_i,\\ \dot{z}_i &= f + z_i(x_i - c),\end{aligned} \tag{35}$$

where a, f, c, and ω are system parameters. The phase dynamics of the system, with some approximations, can be reduced to the Kuramoto case [26]. In a phase coherent regime, the amplitude and phase of the oscillators can be defined by introducing the variables $A_i = \sqrt{x_i^2 + y_i^2}$ and $\Phi_i = \arctan(y_i/x_i)$ [27,28]. The dynamics of the system in terms of A, Φ, and z is then given by

$$\begin{aligned}\dot{A}_i &= a A_i \sin^2\Phi_i - z_i\cos\Phi_i + \frac{\varepsilon}{k_i}\sum_{j=1}^{N} a_{ij}\\ &\quad\times (A_j(t-\tau)\cos\Phi_j(t-\tau)\cos\Phi_i - A_i\cos^2\Phi_i),\\ \dot{\theta}_i &= \omega + a\sin\Phi_i\cos\Phi_i\\ &\quad + \frac{z_i}{A_i}\sin\Phi_i - \frac{\varepsilon}{k_i}\sum_{j=1}^{N} a_{ij}\\ &\quad\times\left(\frac{A_j(t-\tau)}{A_i}\cos\Phi_j(t-\tau)\sin\Phi_i - \sin\Phi_i\cos\Phi_i\right),\\ \dot{z}_i &= f - c z_i + A_i z_i\cos\Phi_i\end{aligned} \tag{36}$$

for $i = 1,2,\ldots,N$. We analyze the system by averaging over the rotations of the phases Φ_i [27,29]. Assuming that the amplitudes vary slowly, new slow phases φ_i can be introduced through the substitution $\Phi_i = \omega_0 t + \varphi_i$. Averaging the equations we get

$$\begin{aligned}\omega_0 + \dot{\varphi}_i &= \omega + \frac{\varepsilon}{k_i}\sum_{j=1}^{N} a_{ij}\\ &\quad\times\left(\frac{A_j(t-\tau)}{2A_i}\sin[\varphi_j(t-\tau) - \varphi_i(t) - \omega_0\tau]\right).\end{aligned} \tag{37}$$

The substitution $\varphi_i(t) = \theta_i(t) - \omega_0 t$ transforms these equations to a corotating frame of frequency ω_0 and we find

$$\dot{\theta}_i = \omega + \frac{\varepsilon}{k_i}\sum_{j=1}^{N} a_{ij}\frac{A_j(t-\tau)}{2A_i}\sin[\theta_j(t-\tau) - \theta_i(t)]. \tag{38}$$

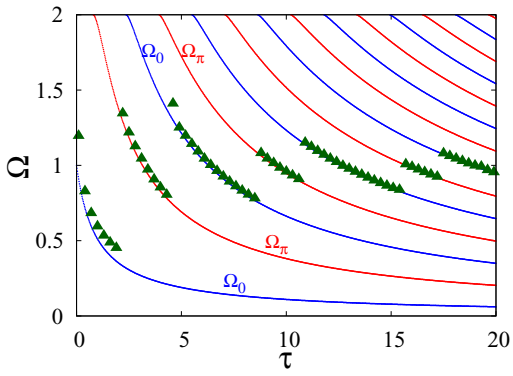

FIG. 11. (Color online) Rössler oscillators on a bipartite network (again with $N_A = N_B = 3$ and $a = 0.2$, $f = 0.2$, $c = 1.0$, and $\omega = 1.0$ taken for the numerics). The green triangles are the numerically calculated frequencies from the system (35) at coupling strength $\varepsilon = 2.0$. The blue and red lines (indicated by Ω_0 and Ω_π) are, respectively, the in-phase and antiphase frequencies for the systems calculated from the transcendental equation (40) at equivalent coupling strength $K = \varepsilon/2 = 1$.

Under the assumption that $A_i \approx A_j\ \forall i,j$, the equations for phases can be written as

$$\dot{\theta}_i = \omega + \frac{K}{k_i}\sum_{j\in B} a_{ij}\sin[\theta_j(t-\tau) - \theta_i(t)], \tag{39}$$

where $K = \varepsilon/2$. Note that this reduced equation is similar to that of Landau-Stuart oscillators (34), the only difference being that the effective coupling strength K is reduced by a factor of 2. With this in mind, the analysis of previous sections is applicable and the collective frequency Ω now satisfies the

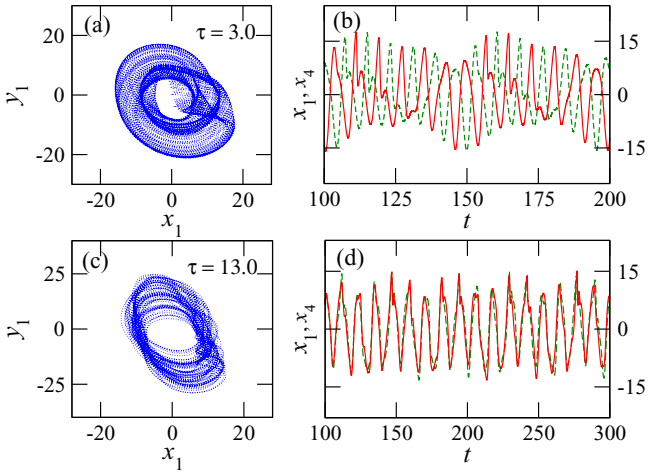

FIG. 12. (Color online) Identical Rössler oscillators in the chaotic regime $a = 0.2, f = 0.2, c = 9.0, \omega = 1.0$ for coupling strength $\varepsilon = 2$. The attractor in the x-y plane for one of the oscillators is plotted for delays (a) $\tau = 3.0$ and (c) $\tau = 13.0$. The variable $x(t)$ for oscillators $i = 1 \in A$ (solid red) and $i = 4 \in B$ (dashed green) are plotted in (b) and (d) as a function of time. (b) At $\tau = 3.0$, the oscillators from different partitions are in antiphase synchrony and (d) at $\tau = 13.0$, oscillators are in-phase synchronized. There are three oscillators in each partition, $N_A = N_B = 3$.

equation [cf. Eq. (20)]

$$\Omega_{0,\pi} = \omega \mp \frac{\varepsilon}{2} \sin(\Omega_{0,\pi}\tau). \tag{40}$$

Figure 11 shows that the values of the collective frequency calculated from Eq. (40) are in good agreement with numerical results in the periodic regime (parameter $c = 1.0$). Similarly, the regions of phase space when the coupled system settles into in-phase or antiphase synchrony can be estimated via the above analysis. Even though the frequency estimation for the chaotic case ($c = 9.0$) is not straightforward, we still can observe the in-phase and antiphase behavior in the chaotic time series at two different delays, as shown in Fig. 12.

VI. CONCLUSION

Bipartite topologies are frequently encountered in a variety of naturally occurring networks. We have studied the dynamics of identical oscillators that are coupled with distributed time delays in such a geometry and examined the different phase-locked regimes that can arise. There are two resultant stable configurations when the system is in synchrony. Although the oscillators evolve to a common collective frequency, between the partitions there can be a phase difference of either 0 or π radians. These are the *only* possible phase-locked solutions in bipartite networks of identical oscillators. We have analyzed general bipartite networks with distributed coupling delays, established the existence of these two kinds of solutions, and derived conditions for their stability.

A consequence of the time delay is that there can be more than one stable oscillation frequency; multistability is therefore frequently encountered with such coupling. We have shown that the number of stable solutions increase linearly with increasing delay or with increasing coupling strength. The system can then exhibit hysteresis and sensitivity to disturbances and the collective frequency jumps to a different value or the phase difference between the partitions switches between 0 and π, as the system moves from one attractor to another. There is the further possibility of synchronizing to any frequency in a certain interval by choosing an appropriate delay. Results have been presented for simple phase oscillators, for which the analysis is exact, as well as paradigmatic examples such as Landau-Stuart and Rössler oscillators, whose phase dynamics can be reduced to the Kuramoto model under appropriate conditions. In all these examples, analytical and numerical results are in very good agreement.

Several studies have focused on understanding collective behavior of oscillators on various types of networks, both with and without time delay. In addition to the phenomenon seen here, namely, the separation of the network into groups of individually phase-synchronized oscillators, there are a variety of other possible dynamical states [23] and even within the framework of bipartite topology it is clear that more general situations need to be addressed. For example, the role of heterogeneity, both in the individual oscillators and in the coupling, needs to be investigated. The manner in which departures from this topology, for instance, the introduction of a few additional connections, modifies these results is also of interest. These and similar questions have been investigated in Ref. [30].

ACKNOWLEDGMENTS

N.P. and R.R. thank the Department of Science and Technology, India for research support. N.P. would also like to acknowledge the kind hospitality of the MPI-MIS, Leipzig. F.M.A. acknowledges support from European Union's Seventh Framework Programme (FP7/2007-2013) under Grant No. 318723 (MatheMACS).

[1] H. Jeong, B. Tombor, R. Albert, Z. N. Oltvai, and A.-L. Barabási, Nature (London) **407**, 651 (2000).
[2] M. E. J. Newman, Proc. Natl. Acad. Sci. USA **98**, 404 (2001).
[3] P. Holme, F. Liljeros, C. R. Edling, and B. J. Kim, Phys. Rev. E **68**, 056107 (2003).
[4] J. Ohkubo, K. Tanaka, and T. Horiguchi, Phys. Rev. E **72**, 036120 (2005).
[5] J. L. Guillaume and M. Latapy, Physica A **371**, 795 (2006).
[6] S. Saavedra, F. R. Tsochas, and B. Uzzi, Nature (London) **457**, 463 (2009).
[7] K. Sneppen, M. Rosvall, A. Trusina, and P. Minnhagen, Europhys. Lett. **67**, 349 (2004).
[8] S. H. Strogatz, Nature (London) **410**, 268 (2001).
[9] E. Schöll, Nat. Phys. **6**, 161 (2010).
[10] R. Albert and A.-L. Barabási, Rev. Mod. Phys. **74**, 47 (2002).
[11] M. Nixon, M. Friedman, E. Ronen, A. A. Friesem, N. Davidson, and I. Kanter, Phys. Rev. Lett. **108**, 214101 (2012); **106**, 223901 (2011).
[12] J. Zamora-Munt, C. Masoller, J. Garcia-Ojalvo, and R. Roy, Phys. Rev. Lett. **105**, 264101 (2010); M. Bennett *et al.*, Proc. R. Soc. London Ser. A **458**, 563 (2002); D. McMillen *et al.*, Proc. Natl. Acad. Sci. USA **99**, 679 (2002); J. Garcia-Ojalvo *et al.*, *ibid.* **101**, 10955 (2004); C. L. Tang *et al.*, J. Appl. Phys. **34**, 2289 (1963); K. Wiesenfeld, C. Bracikowski, G. James, and R. Roy, Phys. Rev. Lett. **65**, 1749 (1990).
[13] W. Singer, Neuron **24**, 49 (1999); P. A. Tass *et al.*, Phys. Rev. Lett. **81**, 3291 (1998); C. Masoller, M. C. Torrent, and J. Garcia-Ojalvo, Philos. Trans. R. Soc. London Ser. A **367**, 3255 (2009).
[14] R. Vardi, A. Wallach, E. Kopelowitz, M. Abeles, S. Marom, and I. Kanter, Europhys. Lett. **97**, 66002 (2012).
[15] I. Fischer, R. Vicente, J. M. Buldu, M. Peil, C. R. Mirasso, M. C. Torrent, and J. Garcia-Ojalvo, Phys. Rev. Lett. **97**, 123902 (2006).
[16] L. M. Pecora and T. L. Carroll, Phys. Rev. Lett. **80**, 2109 (1998); V. Flunkert, S. Yanchuk, T. Dahms, and E. Schöll, *ibid.* **105**, 254101 (2010); V. Flunkert and E. Schöll, New J. Phys. **14**, 033039 (2012).
[17] M. K. S. Yeung and S. H. Strogatz, Phys. Rev. Lett. **82**, 648 (1999).
[18] M. G. Earl and S. H. Strogatz, Phys. Rev. E **67**, 036204 (2003).
[19] Y. Kuramoto, *Chemical Oscillations, Waves and Turbulence* (Springer, Berlin, 1984); H. Sakaguchi and Y. Kuramoto, Prog. Theor. Phys. **76**, 576 (1986); Y. Kuramoto, Physica D **50**, 15

(1991); S. K. Han, C. Kurrer, and Y. Kuramoto, Phys. Rev. Lett. **75**, 3190 (1995).

[20] J. D. Crawford, J. Stat. Phys. **74**, 1047 (1994); Phys. Rev. Lett. **74**, 4341 (1995).

[21] H. G. Schuster and P. Wagner, Prog. Theor. Phys. **81**, 939 (1989).

[22] D. S. Goldobin and A. Pikovsky, Prog. Theor. Phys. Suppl. **161**, 43 (2006).

[23] Y. Kuramoto and D. Battogtokh, Nonlinear Phenom. Complex Syst. (Minsk, Belarus) **5**, 380 (2002); D. M. Abrams and S. H. Strogatz, Phys. Rev. Lett. **93**, 174102 (2004).

[24] G. C. Sethia, A. Sen, and F. M. Atay, Phys. Rev. Lett. **100**, 144102 (2008).

[25] F. M. Atay, Philos. Trans. R. Soc. London Ser. A **371**, 20120460 (2013).

[26] N. Punetha, R. Karnatak, A. Prasad, J. Kurths, and R. Ramaswamy, Phys. Rev. E **85**, 046204 (2012).

[27] A. Pikovsky, M. Rosenblum, and J. Kurths, *Synchronization, A Universal Concept in Nonlinear Science* (Cambridge University Press, Cambridge, 2001).

[28] The phase variable for the Rössler system [27] is defined by choosing a Poincaré surface, with a transversally crossing trajectory gaining 2π for every return to this surface of section. We estimate the phase of the system by introducing angle variable via transformation to the polar coordinates. When the coupled system is periodic or in the amplitude death region, the projection of the phase portrait on the (x,y) plane has well-defined rotations around a fixed point. However, for some parameter values it is difficult to find a line in the (x,y) plane that is transversally crossed by all trajectories. Also, if the behavior of the coupled system has several different time scales of oscillations, then it is difficult to decide which waveform should be considered as a cycle and assigned to the 2π increase in phase. For such situations the phase is ill defined [27] and therefore the simple phase reduction procedure cannot be applied and other definitions are needed.

[29] M. G. Rosenblum, A. S. Pikovsky, and J. Kurths, Phys. Rev. Lett. **78**, 4193 (1997).

[30] N. Punetha, S. R. Ujjwal, F. M. Atay, and R. Ramaswamy, Phys. Rev. E **91**, 022922 (2015).